9306–9315 *Nucleic Acids Research, 2011, Vol. 39, No. 21* *Published online 3 August 2011*
doi:10.1093/nar/gkr619

Gln-tRNA^{Gln} synthesis in a dynamic transamidosome from *Helicobacter pylori*, where GluRS2 hydrolyzes excess Glu-tRNA^{Gln}

Jonathan L. Huot[1], Frédéric Fischer[2], Jacques Corbeil[3], Éric Madore[3], Bernard Lorber[2], Guillaume Diss[2], Tamara L. Hendrickson[4], Daniel Kern[2,*] and Jacques Lapointe[1,*]

[1]Département de Biochimie, de Microbiologie et de Bio-informatique, PROTEO et IBIS, Université Laval, 1045 av. de la Médecine, Québec (Québec), Canada, G1V 0A6, [2]Institut de Biologie Moléculaire et Cellulaire, UPR 9002 du CNRS, Architecture et Réactivité de l'ARN, Université de Strasbourg, 15 rue René Descartes, 67084 Strasbourg Cedex, France, [3]Département de Médecine Moléculaire, Université Laval, Centre Hospitalier Universitaire de Québec (Pavillon CHUL), 2705 boul. Laurier, Québec (Québec), Canada, G1V 4G2 and [4]Department of Chemistry, Wayne State University, Detroit, MI 48202, USA

Received January 25, 2011; Revised July 13, 2011; Accepted July 14, 2011

ABSTRACT

In many bacteria and archaea, an ancestral pathway is used where asparagine and glutamine are formed from their acidic precursors while covalently linked to tRNA^{Asn} and tRNA^{Gln}, respectively. Stable complexes formed by the enzymes of these indirect tRNA aminoacylation pathways are found in several thermophilic organisms, and are called transamidosomes. We describe here a transamidosome forming Gln-tRNA^{Gln} in *Helicobacter pylori*, an ε-proteobacterium pathogenic for humans; this transamidosome displays novel properties that may be characteristic of mesophilic organisms. This ternary complex containing the non-canonical GluRS2 specific for Glu-tRNA^{Gln} formation, the tRNA-dependent amidotransferase GatCAB and tRNA^{Gln} was characterized by dynamic light scattering. Moreover, we observed by interferometry a weak interaction between GluRS2 and GatCAB (K_D = 40 ± 5 μM). The kinetics of Glu-tRNA^{Gln} and Gln-tRNA^{Gln} formation indicate that conformational shifts inside the transamidosome allow the tRNA^{Gln} acceptor stem to interact alternately with GluRS2 and GatCAB despite their common identity elements. The integrity of this dynamic transamidosome depends on a critical concentration of tRNA^{Gln}, above which it dissociates into separate GatCAB/tRNA^{Gln} and GluRS2/tRNA^{Gln} complexes. Ester bond protection assays show that both enzymes display a good affinity for tRNA^{Gln} regardless of its aminoacylation state, and support a mechanism where GluRS2 can hydrolyze excess Glu-tRNA^{Gln}, ensuring faithful decoding of Gln codons.

INTRODUCTION

Survival in a competitive environment requires a high degree of faithfulness in protein biosynthesis to avoid not only lethal mutations but also those affecting fitness. Decoding of genetic information typically takes place on highly specific enzymes named aminoacyl-tRNA synthetases (aaRSs). Even though there are aaRSs for all 20 canonical amino acids, half of all characterized bacteria and archaea are deprived of asparaginyl-tRNA synthetase (AsnRS). Similarly, glutaminyl-tRNA synthetase (GlnRS) is absent from all archaea and most bacteria (1–3).

The indirect pathway used for the formation of Gln-tRNA^{Gln} was discovered in 1968 by Wilcox and Nirenberg (4). The first enzyme in this pathway is a non-discriminating aaRS (ND-aaRS) such as the ND-GluRS of *Bacillus subtilis*, which glutamylates both tRNA^{Glu} and tRNA^{Gln}, or a non-canonical GluRS2 such as those of *Helicobacter pylori* and *Acidithiobacillus ferrooxidans*, which glutamylate only tRNA^{Gln} (5–7). The second enzyme of this pathway is an aminoacyl-tRNA

*To whom correspondence should be addressed. Tel: +1 418 656 2131, extn 3411; Fax: +1 418 656 3664; Email: jacques.lapointe@bcm.ulaval.ca
Correspondence may also be addressed to Daniel Kern. Tel: +33 0 3 88 41 70 92; Fax: +33 0 3 88 60 22 18; Email: d.kern@ibmc.u-strasbg.fr

The authors wish it to be known that, in their opinion, the first two authors should be regarded as joint First Authors.

amidotransferase, such as the trimeric GatCAB of *B. subtilis*, which transamidates Glu-tRNA^{Gln} into Gln-tRNA^{Gln} (8). GatCAB also catalyzes the indirect pathway for the formation of Asn-tRNA^{Asn}, when an ND-AspRS is present to provide the Asp-tRNA^{Asn} substrate (9). The formation of these misacylated aa-tRNAs must not lead to translational errors. To this end, several strategies have evolved, such as the proofreading activities of aaRSs (10), and the discrimination by elongation factor EF-Tu against misacylated tRNAs through thermodynamic compensation (11). ND-GluRS and ND-AspRS possess no proofreading activities, but Asp-tRNA^{Asn} and Glu-tRNA^{Gln} are deprived of significant affinity for EF-Tu (12,13). Despite this, *in vivo* experiments have shown that under certain conditions, the Glu residue of Glu-tRNA^{Gln} can be incorporated into proteins, suggesting that an additional locking mechanism may be needed to prevent translational errors (6,14). Such a mechanism was shown in *Pseudomonas aeruginosa* and *H. pylori*, where the channeling of misacylated aa-tRNAs from the ND-aaRS to the aa-tRNA amidotransferase effectively sequesters them (15), as initially suggested by Schön *et al.* (16). Sequestration of misacylated aa-tRNAs through the formation of more robust interactions was then confirmed in thermophilic organisms. These were first described in *Thermus thermophilus*, where ND-AspRS, tRNA^{Asn} and GatCAB form a ternary complex for the biosynthesis of Asn-tRNA^{Asn} (17,18). A ternary complex for the formation of Gln-tRNA^{Gln} was then described for *Methanothermobacter thermoautotrophicus*, involving ND-GluRS, the archaeal amidotransferase GatDE, and tRNA^{Gln} (19). Although they differ in their mode of assembly, both complexes were named transamidosomes, in reference to their activity: the archaeal Gln-transamidosome is formed by a tight ND-GluRS/GatDE complex ($K_D = 100$ nM) which then binds tRNA^{Gln}, whereas the *T. thermophilus* Asn-transamidosome assembles through ND-AspRS and GatCAB binding to tRNA^{Asn} without any protein–protein interactions. These transamidosomes are similar to the complex catalyzing Cys-tRNA^{Cys} biosynthesis in *Methanocaldococcus jannaschii* (20), suggesting that formation of complexes for tRNA-dependent amino acid biosynthesis is the norm in thermophilic organisms. In agreement with this is the structural data obtained with *Thermotoga maritima* ND-GluRS, tRNA^{Gln} and GatCAB in a ternary complex assisted by a covalent linkage of the GatC subunit to ND-GluRS, which demonstrates that no steric hindrances prevent the simultaneous binding of GatCAB and a GluRS to tRNA^{Gln} (21).

In this work, we describe a Gln-tRNA^{Gln} synthesizing ternary complex in *H. pylori*, suggesting that the transamidosome model extends to mesophilic organisms. *H. pylori* GatCAB and GluRS2 bind to tRNA^{Gln} and are further stabilized by a weak interaction directly between GluRS2 and GatCAB. The *H. pylori* Gln-transamidosome is less stable than those previously described. This fluidity enables conformational changes which allow both enzymes to alternately bind their shared identity elements on the tRNA^{Gln} acceptor stem.

MATERIALS AND METHODS

Overproduction and purification of enzymes and tRNA^{Gln}

Cells for the overproduction of *H. pylori* GluRS2 and GatCAB were cultured and lysed as adapted from previous works (6,15). Both enzymes were purified by ion-exchange chromatography on DEAE-cellulose (DE52, Whatman), followed by affinity chromatography on Ni-NTA resin (Novagen). Enzymes used for kinetic measurements were additionally purified by gel-filtration on a Superdex 200 HR 10/30 column (Amersham). The *H. pylori* tRNA^{Gln} gene, cloned into the pES300 plasmid (6), was overexpressed in *Escherichia coli* DH5α, and tRNA^{Gln} was purified as previously described (22); it was eluted between 0.9 and 0.6 M of $(NH_4)_2SO_4$ on Sepharose-4B, between 20 and 300 mM potassium phosphate on hydroxyapatite (Bio-Rad), and between 0.5 and 1.0 M NaCl on a MonoQ HR10/100 column (GE Healthcare). Fractions of between 40 and 83% pure tRNA^{Gln} were obtained.

Gel-filtration

Experiments were conducted as described (22), using an ÄKTA Purifier and a 24-ml Superdex G200 column (GE Healthcare). Na–HEPES buffer (50 mM, pH 7.2) was used, containing 30 mM KCl, 6 mM $MgCl_2$, 0.1 mM Na_2-EDTA and 5 mM 2-mercaptoethanol, at 12°C. K_D values ([free enzyme] × [free tRNA^{Gln}]/[enzyme–tRNA^{Gln} complex]) were determined by evaluating the area of enzyme-bound tRNA and free tRNA peaks, the sum of which equals the total tRNA present in the sample. The contaminating non-specific tRNA (~18%) was subtracted from free tRNA. The quantity of free enzyme was determined by subtracting the quantity of enzyme-bound tRNA from the total amount of enzyme present in the sample.

Dynamic light scattering

DLS measurements were performed as described (22), at 20 ± 0.1°C in a Zetasizer NanoS instrument (Malvern, UK). The 20–40 µl samples contained 20 µM protein with or without tRNA^{Gln} in the gel-filtration buffer. For the titration experiments, the concentrations of two partners was constant and that of the third (GatCAB or tRNA^{Gln}) varied as indicated. Hydrodynamic diameters were corrected for solvent refractive index ($n = 1.3353$) and absolute viscosity ($\eta = 1.041$ mPa.s).

Aminoacylation of tRNA

The reaction mixture contained 100 mM Na–HEPES pH 7.2, 30 mM KCl, 12 mM $MgCl_2$, 2 mM ATP, 20–50 µM [^{14}C]L-Glu (330 cpm pmol^{-1}, GE Healthcare), 0.1 mg ml^{-1} bovine serum albumin, 10 µM of *H. pylori* tRNA^{Gln} and 0.025–0.5 µM *H. pylori* GluRS2. A concentration of 200 µM [^{14}C]L-Glu was used to investigate the rate-limiting step. For K_M measurements of GluRS2 with or without GatCAB, the tRNA^{Gln} concentration varied from 0.1 to 10 µM and that of L-Glu from 50 to 600 µM. Experiments were conducted at 37°C for steady-state measurements, or at 4°C with 10 or 20% glycerol for

pre-steady state measurements. The [^{14}C] aa-tRNA formed in 10 or 20 µl aliquots withdrawn at various time intervals was determined as previously described (23).

ATP-PP$_i$ exchange

The reaction mixture contained 100 mM Na–HEPES pH 7.2, 10 mM $MgCl_2$, 5 µM $tRNA^{Gln}$, 2 mM L-Glu, 2 mM ATP, 2 mM [^{32}P]PP$_i$ (2 cpm/pmol, PerkinElmer) and 0.5 µM GluRS2. The formation of [^{32}P]ATP at 37°C was followed at various time intervals in 40 µl aliquots, as previously described (23).

Gln-$tRNA^{Gln}$ formation

Reactions were performed in a mixture containing 50 mM Na–HEPES pH 7.2, 30 mM KCl, 12 mM $MgCl_2$, 2 mM ATP, 1.28 mM L-Gln and 1 mM dithiothreitol. An amount of 50 µM [^{14}C]L-Glu was added to the reaction mixture for glutamylation–transamidation experiments. For experiments measuring only transamidation, GatCAB was used at a concentration of 15 nM, while GluRS2 was used at 6.6 µM when it was in excess. The Glu-$tRNA^{Gln}$ substrate was synthesized separately, and purified as described (15). For reactions where glutamylation and transamidation were measured simultaneously, an equimolar concentration of GatCAB and GluRS2 (50 nM), and uncharged $tRNA^{Gln}$ at various concentrations were used. Both kinds of experiment were performed at 37°C, with 10 µl reaction aliquots prepared and then analyzed by migration on cellulose thin-layer chromatography plates as previously described (24). Product formation was quantified using radioactivity standards (15).

Stability of Glu-$tRNA^{Gln}$ and Gln-$tRNA^{Gln}$

Both aa-tRNAs were purified as described above, with Gln-$tRNA^{Gln}$ formed by subjecting Glu-$tRNA^{Gln}$ to a transamidation step in the presence of GatCAB before extraction and precipitation. Half-lives were then measured in the transamidation reaction mixture with ATP and Gln excluded, as previously described (15).

Detection of macromolecular interactions by nanopore optical interferometry (NpOI)

These interactions were measured in a Ski Pro NpOI instrument (Silicon Kinetics), using carboxy-functionalized silicon biosensor chips containing covalently-bound GluRS2, GatCAB or GluRS1. These were prepared as previously described (25) using protein concentrations of 0.25, 0.25 and 0.5 mg ml^{-1}, respectively. Assayed against these biosensor chips were target proteins diluted to various concentrations in the buffer used for gel-filtration. To obtain binding data, the target protein was injected into the sample channel of the biosensor chip for 300 s, while the binding buffer was injected into the reference channel. To obtain the dissociation data, binding buffer was injected into the sample channel in addition to the reference channel for at least 100 s to trigger the mass dilution of the target protein. In both cases, the optical path difference of the reference channel was subtracted from that of the sample channel.

RESULTS

Helicobacter pylori GluRS2 and GatCAB have comparable affinities for $tRNA^{Gln}$

An important characteristic of previously described transamidosomes is that the GatCAB and the aaRS can both bind $tRNA^{Gln}$ or $tRNA^{Asn}$ (17,19). We therefore used gel-filtration to investigate the capacity of GluRS2 and GatCAB to form binary complexes with $tRNA^{Gln}$. GluRS2 binds to *Hp* $tRNA^{Gln}$ with a K_D value estimated at 2 ± 0.6 µM (Figure 1A). In accordance with previous observations, GatCAB also made a complex with uncharged $tRNA^{Gln}$ with a K_D value of 4 ± 1 µM (Figure 1B), close to that measured for GluRS2. No ternary complex was detected, either using $tRNA^{Gln}$ or Glu-$tRNA^{Gln}$, whether the latter was simultaneously formed, or prepared in advance (Figure 1C and D). Direct protein–protein interactions were also undetectable by gel-filtration, as seen when comparing elution volumes of GluRS2 and GatCAB (Figure 1A, B and C). As the free and bound forms of these macromolecules are not at equilibrium during gel-filtration, these results do not rule out the existence of a ternary complex, nor of a direct GluRS2/GatCAB interaction, and they imply that the K_D values obtained are upper limits.

Characterization of GluRS2/GatCAB interactions by nanopore optical interferometry (NpOI)

Gel-filtration experiments indicated that if a Gln-transamidosome exists in *H. pylori*, it would be more unstable than those previously described. Nevertheless, we attempted to determine if protein–protein interactions occur, as is the case for the *M. thermoautotrophicus* Gln-transamidosome (19). Using NpOI, we measured the quantity of GatCAB bound by a GluRS2 biosensor chip, for increasing GatCAB concentrations in a mobile phase (Figure 2A). Dissociation of the GatCAB from the biosensor chip was measured by injecting buffer. Using the detected amounts of GluRS2-bound GatCAB at equilibrium, we determined a K_D of 40 ± 5 µM for the GluRS2/GatCAB complex (Figure 2B) (26). Using the dissociation equation for the reversible binding of two molecules (27), we calculated a k_{off} of 0.12 s^{-1} for the dissociation of this complex, which together with the K_D value, yields a k_{on} of 0.003 s^{-1} µM^{-1}. Control experiments using GatCAB, GluRS2, and the discriminating *H. pylori* GluRS1 in various combinations revealed minimal binding between GluRS1 and GluRS2, between GluRS1 and GatCAB and between GluRS1 and GluRS1 itself (Figure 2C). Although we obtained data for the binding of GluRS2 to fixed GatCAB, the ability of GluRS2 to bind to itself (Figure 2C) interfered with data interpretation.

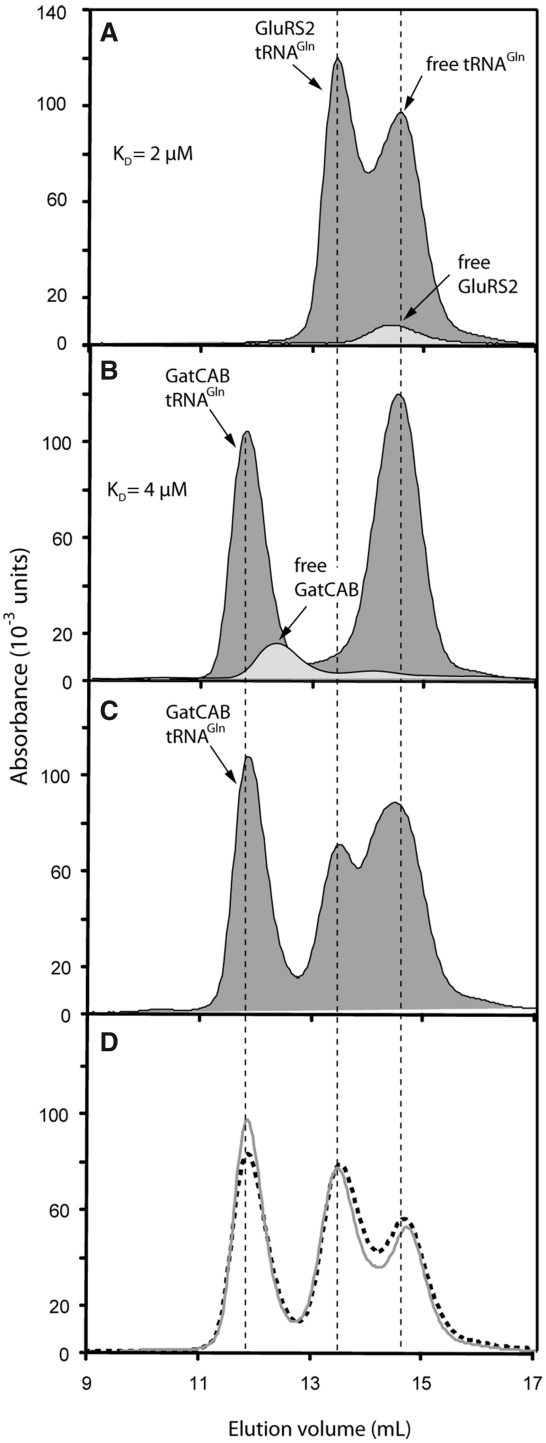

Figure 1. Binding experiments with $tRNA^{Gln}$, GluRS2 and GatCAB as shown by size-exclusion chromatography. (**A**) Comparison of isolated GluRS2 and GluRS2/$tRNA^{Gln}$ complex profiles. The association enabled us to estimate a K_D value for GluRS2 and $tRNA^{Gln}$ binding (see 'Materials and Methods' section). (**B**) Comparison between free and $tRNA^{Gln}$-complexed GatCAB. (**C**) Gel-filtration of a solution containing the three partners. (**D**) The same experiment as described in (C) was performed with preformed Glu-$tRNA^{Gln}$ (grey line) or after incubation of the three partners within an aminoacylation medium containing free Glu and ATP, to provide endogenous Glu-$tRNA^{Gln}$ (dotted line). Proteins and $tRNA^{Gln}$ were added at concentrations of 20 µM each for the experiments shown in all panels.

Characterization of a ternary complex of GluRS2/$tRNA^{Gln}$/GatCAB by dynamic light scattering (DLS)

The GluRS2/$tRNA^{Gln}$, GatCAB/$tRNA^{Gln}$ and GluRS2/GatCAB binary complexes detected by gel-filtration (Figure 1) and NPoI (Figure 2B) did not show a significant increase in apparent mean hydrodynamic diameter over those of the free proteins (Figure 3, lanes 1–7). The particle size measured for GluRS2/GatCAB decreased when the concentration of GluRS2 was increased, confirming that this complex was very labile. Finally, we tested the effect of $tRNA^{Gln}$ addition: when the three partners were mixed, a new particle of significantly larger size was formed (Figure 3, lane 8). This shows that while weak GluRS2/GatCAB interactions occur, the strongest interactions in the ternary complex are those between both enzymes and $tRNA^{Gln}$. The apparent mass (259 kDa) deduced from the particle size (12.8 nm) is roughly equal to the sum of those measured for GluRS2/$tRNA^{Gln}$ and GatCAB, or for GatCAB/$tRNA^{Gln}$ and GluRS2.

In order to confirm that this complex is a GluRS2/$tRNA^{Gln}$/GatCAB transamidosome, we performed a titration of an equimolar mix of GluRS2 and GatCAB with free $tRNA^{Gln}$, increasing the molar ratio from 0.3 to 2.5 (Figure 4A, upper panel), and a titration of a equimolar mix of GluRS2 and $tRNA^{Gln}$ with free GatCAB, with molar ratios of 0 to 2 (Figure 4B). Titration with tRNA led to a nearly symmetrical bell-shaped curve, indicating that increasing $tRNA^{Gln}$ concentrations first led to the formation of a GluRS2/$tRNA^{Gln}$/GatCAB ternary complex with a 1/1/1 stoichiometry, and then to separate saturation of both GluRS2 and GatCAB with free $tRNA^{Gln}$ (Figure 4A, lower panel), disrupting the ternary complex. Titration with GatCAB led to a hyperbolic saturation curve (Figure 4B), also indicating a stoichiometry of 1/1/1. The titration of a GatCAB/$tRNA^{Gln}$ stoichiometric mix with GluRS2 gave strong dispersion in hydrodynamic parameters, probably due to the ability of this aaRS to bind to itself (Figure 2C).

Kinetic experiments reveal a model for Gln-$tRNA^{Gln}$ formation in the *H. pylori* glutamine transamidosome

We found that the K_M for Glu and the k_{cat} of the non-canonical GluRS2 (140 ± 26 µM; $0.16 \pm 0.012\ s^{-1}$) are comparable to those of the *B. subtilis* ND-GluRS (28). Because of this high K_M value, GluRS2 aminoacylation kinetic values for $tRNA^{Gln}$ were obtained with a non-saturating concentration of Glu. Each of the two protein partners involved in Gln-$tRNA^{Gln}$ formation altered the kinetic constants of the other. The presence of 6.6 µM GatCAB increased the K_M of GluRS2 for $tRNA^{Gln}$ by a factor of 2.1 (Table 1). Similarly, the presence of 6.6 µM GluRS2 increased the K_M of GatCAB for Glu-$tRNA^{Gln}$ nearly 4-fold (Table 1). This is consistent with the fact that GluRS2 and GatCAB have a similar affinity for $tRNA^{Gln}$ (Figure 1). It indicates that both GluRS2 and GatCAB can sequester the acceptor stem away from the other, leading to a kinetic competition, as suggested by the 3D structural data for the *T. maritima* Gln-transamidosome (21). Additional support for this competition model is the fact that Glu-$tRNA^{Gln}$ was an

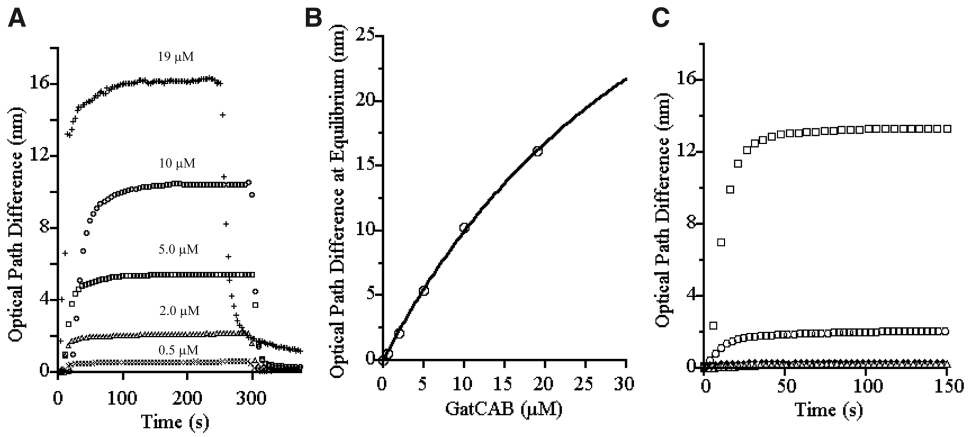

Figure 2. GluRS2–GatCAB interactions characterized by optical interferometry. (**A**) Kinetics of association and dissociation of GatCAB to fixed GluRS2. GatCAB concentrations of 0.5, 2, 5, 10 and 19 μM yielded average optical path differences of 0.6, 2.2, 5.4, 10.4 and 16.2 nm at each plateau. The standard deviation of these averages was <1%. (**B**) Curve of GatCAB bound to GluRS2 at equilibrium (from A) versus the concentration of GatCAB in the mobile phase gives a K_D of 40 ± 5 μM (standard error). The curve was obtained using the equation $Y = L/(K_D + L) \cdot Y_{max}$, where Y is the GatCAB bound at equilibrium, L is its concentration in the mobile phase and Y_{max} the maximum amount of GatCAB bound by the GluRS2 biosensor (26). (**C**) As controls, *H. pylori* GluRS1 was assayed against chip-bound GatCAB (open circle), chip-bound GluRS2 (filled diamond) and chip-bound GluRS1 (open triangle). GluRS1 concentrations of 10, 10 and 40 μM, respectively, were used as the target protein. Binding of GluRS1 with itself or with chip-bound GluRS2 was negligible relative to the ability of GluRS2 to bind to itself (open square). A small amount of GluRS1/GatCAB binding was detected (open circle) but this remained limited compared to the ability of GluRS2 to bind GatCAB (A).

efficient competitive inhibitor of GluRS2, with a K_I value of 1.32 μM (Figure 5) close to the K_M for uncharged $tRNA^{Gln}$ (0.87 μM, Table 1). A concentration of GatCAB equal to that of GluRS2/$tRNA^{Gln}$ allowed formation of a ternary complex, which was not disrupted by the addition of excess GatCAB (Figure 4). This confirms that the effect of an excess of GatCAB on the K_M of GluRS2 for $tRNA^{Gln}$ is not caused by a sequestration of the entire $tRNA^{Gln}$ molecule away from GluRS2, but by competition for the $tRNA^{Gln}$ acceptor stem inside the full-size ternary complex.

Furthermore, GatCAB increased 2.6-fold the aminoacylation k_{cat} of GluRS2 despite the increase in the K_M for $tRNA^{Gln}$ (Table 1). Since dissociation of Glu-$tRNA^{Gln}$ was not rate-limiting (Figure 6), this stimulation by GatCAB can be explained by an effect on the activation of Glu or on its transfer to $tRNA^{Gln}$ in the GluRS2/GatCAB complex. The latter is suggested by the fact that the k_{cat} of the ATP-PP_i exchange reaction monitoring the tRNA-dependent activation of Glu by GluRS2 was one order of magnitude higher ($1.5\,s^{-1}$) than the k_{cat} of the transfer step ($0.16\,s^{-1}$).

Finally, assays were performed measuring glutamylation and transamidation simultaneously using uncharged $tRNA^{Gln}$ and equal concentrations of GluRS2 and GatCAB. Glutamylation occurred with a K_M of 0.69 μM for $tRNA^{Gln}$, and k_{cat} of $0.23\,s^{-1}$, while transamidation occurred with values of 0.97 μM for $tRNA^{Gln}$ and $0.23\,s^{-1}$ (Table 1). Therefore, an equimolar concentration of both enzymes offers the best possible overall rate of Gln-$tRNA^{Gln}$ formation with K_M values nearer to those obtained in the absence of acceptor stem competition. This competition may be the result of inefficient switching between glutamylation and transamidation $tRNA^{Gln}$ binding modes inside the Gln-transamidosome. The overall ternary complex formation could be regulated by the concentration of $tRNA^{Gln}$, for which there would be an optimal cellular concentration for maximum efficiency.

Stability of Glu-$tRNA^{Gln}$ and Gln-$tRNA^{Gln}$

GluRS2 and GatCAB had opposite effects on the stability of the aminoacyl-tRNA link of both of these molecules. GluRS2 reduced 2-fold the half-life of both aa-tRNAs, while GatCAB increased their half-life nearly 5- and 8-fold, respectively (Table 2). Therefore, both enzymes appeared to interact with $tRNA^{Gln}$, regardless of its aminoacylation state, which is consistent with a ternary complex inside which potential competition dictates that neither enzyme should have a greater affinity than the other for the shared substrate. When GluRS2 and GatCAB were both present, no overall deacylation effect was observed (Table 2).

DISCUSSION

The dynamic *H. pylori* glutamine transamidosome

In archaea, Cys-$tRNA^{Cys}$ and Gln-$tRNA^{Gln}$ are synthesized by stable complexes between a misacylating aaRS and a second enzyme providing the final, cognate aa-tRNA (19–21). Our results show that in *H. pylori*, the non-canonical GluRS2 and GatCAB also interact but in a very unstable complex (K_D of 40 ± 5 μM). This is in contrast to the stable complex between ND-GluRS and the archaeal GatDE amidotransferase in *Methanothermobacter thermautotrophicus* (K_D of 100 nM). The weaker complex observed in *H. pylori* may be a result of the absence of an AspRS-like domain in the GatB subunit (19). However, DLS and kinetic

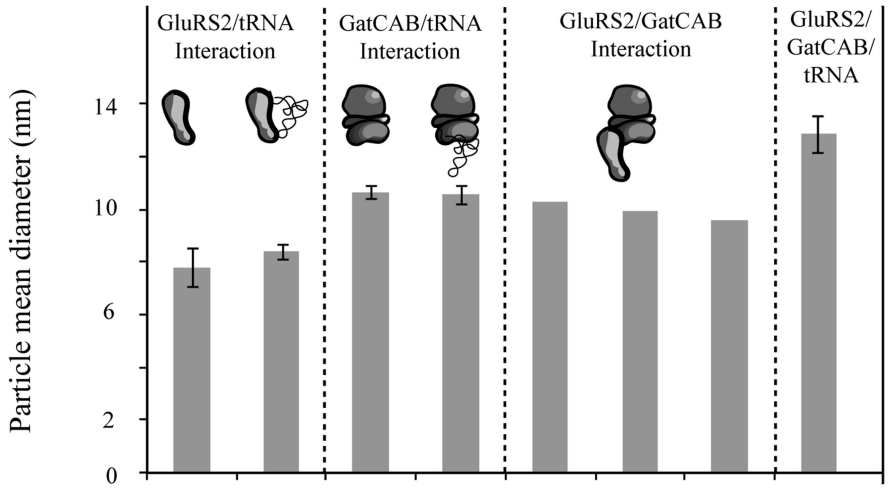

	1	2	3	4	5	6	7	8
GluRS2 (μM)	20	20	-	-	10	20	40	20
GatCAB (μM)	-	-	20	20	20	20	20	20
tRNA (μM)	-	20	-	20	-	-	-	20
Hydrodynamic diameter (nm)	7.8 ± 0.7	8.4 ± 0.3	10.6 ± 0.2	10.6 ± 0.4	10.3	9.9	9.6	12.8 ± 0.7
Apparent Mass (kD)	81 ± 0.3	98 ± 0.0	167 ± 0.0	167 ± 0.1	-	-	-	259 ± 0.3
Real Mass (kD)	50	75	113.6	139	-	-	-	189

Figure 3. Characterization of the ternary complex of glutaminylation by dynamic light scattering. The error bars represent the standard deviation of triplicate experiments. Attempts at detecting GluRS2–GatCAB interactions were performed once, for each of three distinct GluRS2 concentrations.

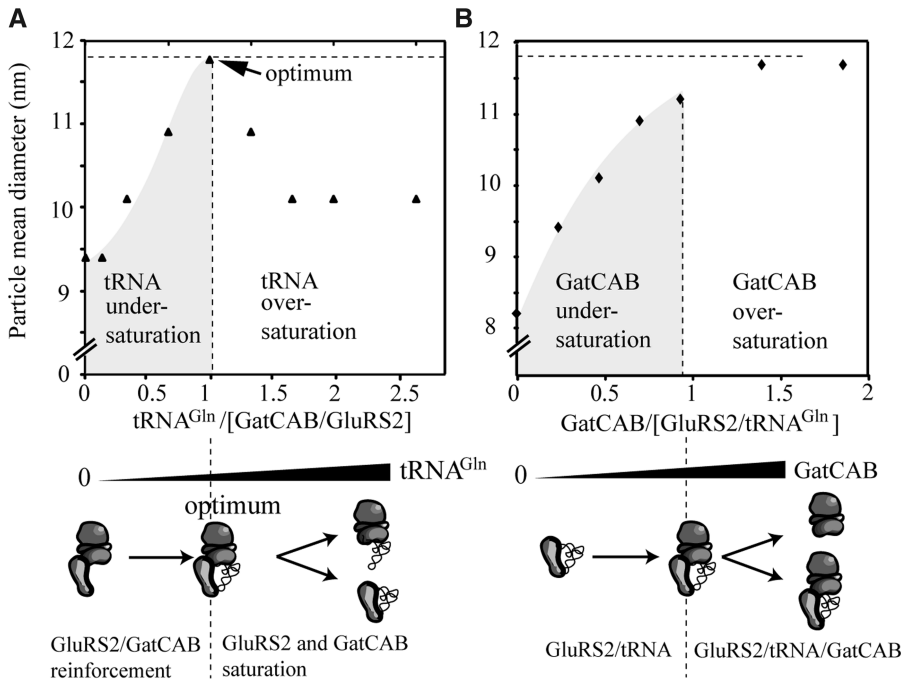

Figure 4. Stoichiometry of the GluRS2/tRNA^{Gln}/GatCAB complex. (**A**) Titration curve of a 1/1 mix of GluRS2 and GatCAB (20 μM each) with tRNA^{Gln} in molar ratios of 0.2–2.7. (**B**) Titration of a 1/1 mix of GluRS2 and tRNA^{Gln} (20 μM each) with free GatCAB in molar ratios of 0.3–2.0.

Table 1. Kinetic constants of GluRS2 for $tRNA^{Gln}$ glutamylation and of GatCAB for Glu-$tRNA^{Gln}$ transamidation in the absence or in the presence of the second protein

	K_M (μM)	k_{cat} (s^{-1})
GluRS2	0.87 ± 0.13	0.094 ± 0.004
GluRS2 + **GatCAB**	1.86 ± 0.19	0.24 ± 0.009
GluRS2 + GatCAB	0.69 ± 0.15	0.23 ± 0.015
GatCAB	0.42 ± 0.11	0.21 ± 0.011
GatCAB + **GluRS2**	1.34 ± 0.38	0.21 ± 0.014
GatCAB + GluRS2	0.97 ± 0.30	0.23 ± 0.019

Constants were measured using the assay for the first enzyme indicated. When present as the second enzyme, GatCAB and GluRS2 were in equimolar amounts (normal font), or in excess 330- and 440-fold, respectively (in bold). Reported K_M values are for $tRNA^{Gln}$ in all experiments except GatCAB alone and with an excess of GluRS2, in which they were for Glu-$tRNA^{Gln}$. Errors shown are the standard errors for non-linear curve-fitting of data obtained from at least two experiments.

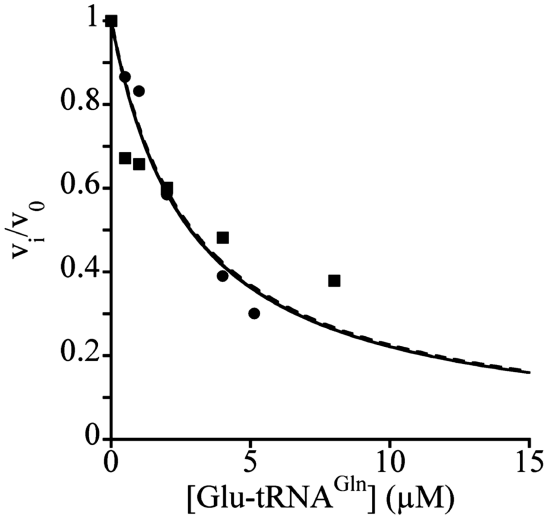

Figure 5. Glu-$tRNA^{Gln}$ is an inhibitor of the aminoacylation reaction catalyzed by GluRS2. Glu-$tRNA^{Gln}$ was formed as described in 'Materials and Methods' section and added to the GluRS2 reaction mixture at concentrations varying from 0 to 7 μM. V_i/V_0 is equal to $2/[2+(I/K_i)]$ when the substrate concentration is equal to its K_M (15). Two independent experiments were conducted (filled square, filled circle) with 1 μM uncharged $tRNA^{Gln}$ as the substrate, yielding an average K_i of 1.3 ± 0.2 μM.

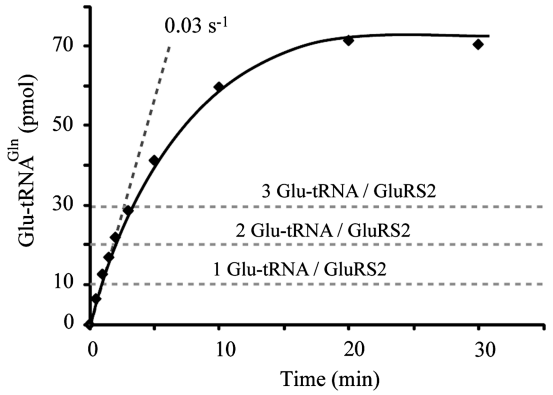

Figure 6. Pre-steady state measurements of Glu-$tRNA^{Gln}$ formation by GluRS2. Aminoacylation reactions were performed at 4°C with 10 μM $tRNA^{Gln}$, and 1 μM GluRS2, taking 10 μl aliquots to measure product formation. No burst indicative of a limiting product-release step was observed.

Table 2. Stability of Glu-$tRNA^{Gln}$ and Gln-$tRNA^{Gln}$

	Half-life (min)	
	Glu-$tRNA^{Gln}$	Gln-$tRNA^{Gln}$
No enzyme	54 ± 1	57 ± 3
GatCAB	245 ± 43	444 ± 111
GluRS2	26 ± 3	26 ± 2
GluRS2 + GatCAB	50 ± 1	55 ± 6

Half-lives for both aa-tRNAs were measured by incubating purified Glu-$tRNA^{Gln}$ or Gln-$tRNA^{Gln}$ in the standard reaction mixture for transamidation, from which Gln and ATP were excluded, at 37°C. When added, proteins were at a concentration of 20 μM. GatCAB protected the ester bond of both aa-tRNAs, while GluRS2 showed a deacylating activity.

experiments have shown that $tRNA^{Gln}$ acts as a scaffold molecule transiently reinforcing the interaction between both GluRS2 and GatCAB which stabilizes the Gln-transamidosome through independent binding of each protein (Figures 3 and 4). The mode of assembly for the *H. pylori* Gln-transamidosome is therefore a hybrid of the protein–RNA mechanism of the *T. thermophilus* Asn-transamidosome, and of the protein–protein mechanism of the Gln-transamidosome of *M. thermoautotrophicus*. The recent structure of the *Thermotoga maritima* Gln-transamidosome reveals that its ND-GluRS and GatCAB can bind simultaneously to a single $tRNA^{Gln}$ molecule (21). The ND-GluRS binds most of the $tRNA^{Gln}$, with the acceptor end within the active site, while the GatB subunit of GatCAB interacts through its C-terminal region with the elbow domain of $tRNA^{Gln}$. Additionally, GluRS2/GatCAB interactions can be seen in the N-terminal regions of both proteins. Consequently, it is possible that GluRS2/$tRNA^{Gln}$ or GatCAB/$tRNA^{Gln}$ complexes can bind the missing partner with a better affinity than either free enzyme, as suggested by the DLS titration experiments (Figure 4). This effect would be similar to the one observed for the binding of aa-AMP or bi-modular inhibitors to aaRSs which are typically more effective than the sum of their parts (29,30).

Our data further refines the *T. maritima* Gln-transamidosome model by experimentally confirming that Glu-$tRNA^{Gln}$ cannot directly flip between both active sites without a rearrangement in the ternary complex structure, but the mechanism we describe differs slightly. The existence of this complex in *H. pylori* depends on a critical concentration of $tRNA^{Gln}$ (Figure 4A) above which the formation of separate binary complexes is favoured, which is not the case for *T. maritima* where a 2:1:1 ratio for $tRNA^{Gln}$/ND-GluRS/GatCAB allowed the formation of a ternary complex detectable by gel-shift

assay [(21) and supplementary information therein]. Excess of the first enzyme over the second increases the K_M of the second enzyme for $tRNA^{Gln}$ (Table 1). An excess of GatCAB does not disrupt the ternary complex (Figure 4B), and therefore induces a conformational change in the complex to the tRNA-binding mode specific to its activity. This may also occur when an excess of GluRS2 is present, but could not be detected by DLS (see above). Such conformational change would be unnecessary if the tRNA acceptor stem was able to flip directly between the catalytic pockets of GluRS2 and GatB.

GluRS2 can hydrolyze excess Glu-$tRNA^{Gln}$

Optimally, upon glutamylation within the Gln-transamidosome, GluRS2 releases the Glu-$tRNA^{Gln}$ acceptor stem towards GatCAB for transamidation before leaving the complex. When this fails to occur, Glu-$tRNA^{Gln}$ may be released without being transamidated and is susceptible to retroactive binding and deacylation by GluRS2 (Figure 5 and Table 2), or could bind to a free GatCAB. Either sequence is possible since Glu-$tRNA^{Gln}$ release is not the rate-limiting step for glutamylation (Figure 6). This mechanism bears a resemblance to the binding and hydrolysis, or resampling, of free Tyr-$tRNA^{Phe}$ by the *E. coli* PheRS which can erroneously synthesize it (31). The GluRS2 resampling-like mechanism (Figure 7) is supported by the fact that aaRSs and their cognate tRNAs are present in similar concentrations within the cell, near the K_M value (32).

The aa-tRNA ester bonds of Glu-$tRNA^{Gln}$ and of Gln-$tRNA^{Gln}$ can be broken by GluRS2, but are protected by GatCAB (Table 2). No net effect on the stability of these aa-tRNAs was observed when both enzymes were present. Asp and Glu are very similar, as are their amidated counterparts, and GatCAB interacts with $tRNA^{Gln}$ and $tRNA^{Asn}$ through the same identity elements. Therefore, these results provide an intriguing contrast to those obtained for the Asn-$tRNA^{Asn}$ forming pathways in *H. pylori* and in *T. thermophilus*, where the individual enzymes (ND-AspRS or AspRS2 and GatCAB) had negligible effects and where the presence of both enzymes had a protective effect on Asn-$tRNA^{Asn}$(15,17).

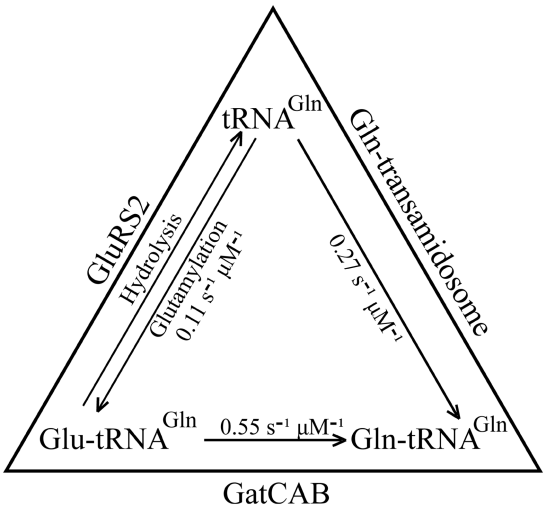

Figure 7. A dynamic system for Gln-$tRNA^{Gln}$ synthesis, which limits free Glu-$tRNA^{Gln}$ in *H. pylori*. The constants shown are the k_{cat}/K_M values calculated from the data in Table 2, for GluRS2 and GatCAB as free enzymes, and for the stoechiometric mix forming the Gln-transamidosome. Starting with $tRNA^{Gln}$, the Gln-transamidosome pathway is favoured, with a k_{cat}/K_M value greater than that of the GluRS2 pathway. Glu-$tRNA^{Gln}$ which is formed outside the Gln-transamidosome is susceptible to deacylation by GluRS2, or to an efficient transamidation by free GatCAB. The entire system therefore regulates against the presence of free Glu-$tRNA^{Gln}$.

Stability of the GluRS2/GatCAB complex

K_D values of several protein–protein interactions are temperature-dependent (33,34). The transamidosomes of thermophilic organisms previously described, and of *H. pylori*, were observed at temperatures between 4°C and room temperature. For the mesophilic *H. pylori* complex, experimental conditions were therefore much less efficient in slowing the normal dynamics.

This lesser stability may also be necessary to leave enough free GatCAB to allow the formation of an Asn-transamidosome: the amidotransferases of both stable transamidosomes described so far, those of *T. thermophilus* and *M. thermoautotrophicus*, catalyze only one activity. On the other hand, the *T. maritima* and *H. pylori* GatCABs fill both transamidation roles in the cell, and may therefore only form unstable Gln-transamidosomes which would facilitate the formation of Asn-transamidosomes. This may be why covalent linkage between ND-GluRS and GatC was needed to obtain structural data for *T. maritima* (21).

A 'loose' association may also be what allows the rearrangements in the complex which are necessary for movement of the acceptor stem. Structural data obtained for GatCAB indicates that the tail domain of GatB responsible for the binding of the D-loop of $tRNA^{Gln}$ is very mobile in relation to the catalytic cradle domain of GatB, which binds the acceptor stem identity element (35). Inside the complex, this flexibility might be what allows contact to be maintained with the D-loop when the cradle domain loses the acceptor stem to GluRS2.

Attempts to characterize the Gln-transamidosome *in vivo*

Attempts were made to detect the complex *in vivo* using the TAP-tag method (36) under conditions where the GluRS2 is overexpressed in *H. pylori* in the presence of physiological concentrations of GatCAB and of $tRNA^{Gln}$. No complex was detected, making it unlikely that an unidentified protein stabilizes the transamidosome. This result is not surprising, given the stringency of the method, which requires that any complexes remain stable over the course of two affinity chromatographies, in order to be detected. The two transamidosomes which have been detected *in vivo* thus far are assembled with affinities of 0.1–0.6 μM (17,19). These experiments required overexpression or high concentrations of all the protein partners in order to isolate the complex. *In vitro*

detection of the *H. pylori* transamidosome, as well as of the *T. maritima* transamidosome (21), required protein concentrations one to two orders of magnitude greater than the affinities above. This suggests that further work is needed to establish the existence of such GluRS/tRNA^{Gln}/GatCAB complexes under physiological conditions, without relying on abnormally high concentrations of some or all partners.

Insights into evolution

In *H. pylori,* translation-targeted Gln is synthesized on a tRNA^{Gln} matrix using the indirect aminoacylation pathway. Such pathways may be remnants of ancient routes for aa-tRNA formation, as suggested by the presence of GatCAB and GluRS in the 'paleome' (37), proposed to include ancestral proteins. EF-Tu can discriminate against mischarged aa-tRNA, such as Asp-tRNA^{Asn}, Glu-tRNA^{Gln} or Ser-tRNA^{Sec} through a thermodynamic compensation mechanism by which aa-tRNAs are most strongly recognized either by their amino acid moiety or their tRNA moiety (11,13). It is probable that this mechanism appeared very early to prevent the use of misacylated tRNAs in protein biosynthesis. Owing to the ancient origin of all aaRSs, it is possible that this property of EF-Tu already existed before GatCAB appeared, and that today's Asp-tRNA^{Asn} and Glu-tRNA^{Gln} escaped early translation, as is the case with some tRNA^{Gly} isoacceptors in *S. aureus* (38). The appearance of Asn- and Gln-transamidosomes provided new aa-tRNAs suitable for EF-Tu binding via the strongly recognized amidated amino acids, leading to a new specification for the present day tRNA^{Gln} (UUG and CUG anticodons) and tRNA^{Asn} (GUU anticodon). Thus, GatCAB, beyond its role in matrix-assisted modifications for amidated aa-tRNA biosynthesis, could also be considered as a codon reassignment enzyme, that led to the present-day genetic code.

ACKNOWLEDGEMENTS

The authors thank Prof. E. Westhof, Dr R. Giegé and Prof. H.D. Becker (IBMC) for support, M. Brayé (IBMC) for technical assistance and Dr H. De Reuse and J. Gallaud (Institut Pasteur, Paris) for performing the TAP-tag experiments.

FUNDING

Natural Sciences and Engineering Research Council of Canada (9597-2010 to J.L.); Fond de Recherche sur la Nature et les Technologies du Québec (PR-105093 to J.L. and graduate fellowship to J.L.H.); Regroupement québecois de recherche sur la fonction, la structure et l'ingénierie des proteines (PROTEO) (graduate fellowship to J.L.H.); Ministère de l'Éducation Nationale, de la Recherche et de la Technologie (graduate fellowship to F.F.); Université de Strasbourg, the Centre National de la Recherche Scientifique and the Association pour la Recherche sur le Cancer (to D.K.); National Institutes of Health (R01GM071480 to T.L.H.). Funding for open access charge: Natural Sciences and Engineering Research Council of Canada (9597-2010).

Conflict of interest statement. None declared.

REFERENCES

1. Feng,L., Sheppard,K., Tumbula-Hansen,D. and Söll,D. (2005) Gln-tRNA^{Gln} formation from Glu-tRNA^{Gln} requires cooperation of an asparaginase and a Glu-tRNA^{Gln} kinase. *J. Biol. Chem.*, **280**, 8150–8155.
2. Kern,D., Roy,H. and Becker,H.D. (2005) In Ibba,M., Francklyn,C. and Cusack,S. (eds), *The Aminoacyl-tRNA Synthetases*. Landes Bioscience, Georgetown, TX, pp. 193–209.
3. Sheppard,K. and Söll,D. (2008) On the evolution of the tRNA-dependent amidotransferases, GatCAB and GatDE. *J. Mol. Biol.*, **377**, 831–844.
4. Wilcox,M. and Nirenberg,M. (1968) Transfer RNA as a cofactor coupling amino acid synthesis with that of protein. *Proc. Natl Acad. Sci. USA*, **61**, 229–236.
5. Lapointe,J., Duplain,L. and Proulx,M. (1986) A single glutamyl-tRNA synthetase aminoacylates tRNA^{Glu} and tRNA^{Gln} in *Bacillus subtilis* and efficiently misacylates *Escherichia coli* tRNA^{Gln1} in vitro. *J. Bacteriol.*, **165**, 88–93.
6. Skouloubris,S., Ribas de Pouplana,L., De Reuse,H. and Hendrickson,T.L. (2003) A noncognate aminoacyl-tRNA synthetase that may resolve a missing link in protein evolution. *Proc. Natl Acad. Sci. USA*, **100**, 11297–11302.
7. Salazar,J.C., Ahel,I., Orellana,O., Tumbula-Hansen,D., Krieger,R., Daniels,L. and Söll,D. (2003) Coevolution of an aminoacyl-tRNA synthetase with its tRNA substrates. *Proc. Natl Acad. Sci. USA*, **100**, 13863–13868.
8. Curnow,A.W., Hong,K., Yuan,R., Kim,S., Martins,O., Winkler,W., Henkin,T.M. and Söll,D. (1997) Glu-tRNA^{Gln} amidotransferase: a novel heterotrimeric enzyme required for correct decoding of glutamine codons during translation. *Proc. Natl Acad. Sci. USA*, **94**, 11819–11826.
9. Curnow,A.W., Tumbula,D.L., Pelaschier,J.T., Min,B. and Söll,D. (1998) Glutamyl-tRNA^{Gln} amidotransferase in *Deinococcus radiodurans* may be confined to asparagine biosynthesis. *Proc. Natl Acad. Sci. USA*, **95**, 12838–12843.
10. Ling,J., Reynolds,N. and Ibba,M. (2009) Aminoacyl-tRNA synthesis and translational quality control. *Annu. Rev. Microbiol.*, **63**, 61–78.
11. LaRiviere,F.J., Wolfson,A.D. and Uhlenbeck,O.C. (2001) Uniform binding of aminoacyl-tRNAs to elongation factor Tu by thermodynamic compensation. *Science*, **294**, 165–168.
12. Stanzel,M., Schön,A. and Sprinzl,M. (1994) Discrimination against misacylated tRNA by chloroplast elongation factor Tu. *Eur. J. Biochem.*, **219**, 435–439.
13. Roy,H., Becker,H.D., Mazauric,M.H. and Kern,D. (2007) Structural elements defining elongation factor Tu mediated suppression of codon ambiguity. *Nucleic Acids Res.*, **35**, 3420–3430.
14. Ruan,B., Palioura,S., Sabina,J., Marvin-Guy,L., Kochhar,S., Larossa,R.A. and Söll,D. (2008) Quality control despite mistranslation caused by an ambiguous genetic code. *Proc. Natl Acad. Sci. USA*, **105**, 16502–16507.
15. Huot,J.L., Balg,C., Jahn,D., Moser,J., Emond,A., Blais,S.P., Chênevert,R. and Lapointe,J. (2007) Mechanism of a GatCAB amidotransferase: aspartyl-tRNA synthetase increases its affinity for Asp-tRNA^{Asn} and novel aminoacyl-tRNA analogues are competitive inhibitors. *Biochemistry*, **46**, 13190–13198.
16. Schön,A., Kannangara,C.G., Gough,S. and Söll,D. (1988) Protein biosynthesis in organelles requires misaminoacylation of tRNA. *Nature*, **331**, 187–190.
17. Bailly,M., Blaise,M., Lorber,B., Becker,H.D. and Kern,D. (2007) The transamidosome: a dynamic ribonucleoprotein particle dedicated to prokaryotic tRNA-dependent asparagine biosynthesis. *Mol. Cell*, **28**, 228–239.
18. Blaise,M., Bailly,M., Frechin,M., Behrens,M.A., Fischer,F., Oliveira,C.L., Becker,H.D., Pedersen,J.S., Thirup,S. and Kern,D.

(2010) Crystal structure of a transfer-ribonucleoprotein particle that promotes asparagine formation. *EMBO J*, **29**, 3118–3129.
19. Rampias,T., Sheppard,K. and Söll,D. (2010) The archaeal transamidosome for RNA-dependent glutamine biosynthesis. *Nucleic Acids Res.*, **38**, 5774–5783.
20. Zhang,C.M., Liu,C., Slater,S. and Hou,Y.M. (2008) Aminoacylation of tRNA with phosphoserine for synthesis of cysteinyl-tRNA^{Cys}. *Nat. Struct. Mol. Biol.*, **15**, 507–514.
21. Ito,T. and Yokoyama,S. (2010) Two enzymes bound to one transfer RNA assume alternative conformations for consecutive reactions. *Nature*, **467**, 612–616.
22. Bailly,M., Blaise,M., Roy,H., Deniziak,M., Lorber,B., Birck,C., Becker,H.D. and Kern,D. (2008) tRNA-dependent asparagine formation in prokaryotes: characterization, isolation and structural and functional analysis of a ribonucleoprotein particle generating Asn-tRNA^{Asn}. *Methods*, **44**, 146–163.
23. Kern,D. and Lapointe,J. (1979) The twenty aminoacyl-tRNA synthetases from *Escherichia coli*. General separation procedure, and comparison of the influence of pH and divalent cations on their catalytic activities. *Biochimie*, **61**, 1257–1272.
24. Bailly,M., Giannouli,S., Blaise,M., Stathopoulos,C., Kern,D. and Becker,H.D. (2006) A single tRNA base pair mediates bacterial tRNA-dependent biosynthesis of asparagine. *Nucleic Acids Res.*, **34**, 6083–6094.
25. Latterich,M. and Corbeil,J. (2008) Label-free detection of biomolecular interactions in real time with a nano-porous silicon-based detection method. *Proteome Sci.*, **6**, 31.
26. Serdyuk,I., Zaccai,N.R. and Zaccai,J. (2007) *Methods in Molecular Biophysics: Structure, Dynamics, Function*. Cambridge University Press, New York, pp. 240–242.
27. Johnson,K.A. (1992) Transient-state kinetic analysis of enzyme reaction pathways. In Sigman,D.S. (ed.), *The Enzymes*, Vol. XX. Academic Press, New York, pp. 1–61.
28. Proulx,M., Duplain,L., Lacoste,L., Yaguchi,M. and Lapointe,J. (1983) The monomeric glutamyl-tRNA synthetase from *Bacillus subtilis* 168 and its regulatory factor. Their purification, characterization, and the study of their interaction. *J. Biol. Chem.*, **258**, 753–759.
29. Lin,S.X., Baltzinger,M. and Remy,P. (1983) Fast kinetic study of yeast phenylalanyl-tRNA synthetase: an efficient discrimination between tyrosine and phenylalanine at the level of the aminoacyladenylate-enzyme complex. *Biochemistry*, **22**, 681–689.
30. Balg,C., Blais,S.P., Bernier,S., Huot,J.L., Couture,M., Lapointe,J. and Chênevert,R. (2007) Synthesis of beta-ketophosphonate analogs of glutamyl and glutaminyl adenylate, and selective inhibition of the corresponding bacterial aminoacyl-tRNA synthetases. *Bioorg. Med. Chem.*, **15**, 295–304.
31. Ling,J., So,B.R., Yadavalli,S.S., Roy,H., Shoji,S., Fredrick,K., Musier-Forsyth,K. and Ibba,M. (2009) Resampling and editing of mischarged tRNA prior to translation elongation. *Mol. Cell.*, **33**, 654–660.
32. Jakubowski,H. and Goldman,E. (1984) Quantities of individual aminoacyl-tRNA families and their turnover in *Escherichia coli*. *J. Bacteriol.*, **158**, 769–776.
33. Banerjee,A., Hu,J. and Goss,D.J. (2006) Thermodynamics of protein-protein interactions of cMyc, Max, and Mad: effect of polyions on protein dimerization. *Biochemistry*, **45**, 2333–2338.
34. Roos,H., Karlsson,R., Nilshans,H. and Persson,A. (1998) Thermodynamic analysis of protein interactions with biosensor technology. *J. Mol. Recognit.*, **11**, 204–210.
35. Nakamura,A., Sheppard,K., Yamane,J., Yao,M., Söll,D. and Tanaka,I. (2010) Two distinct regions in *Staphylococcus aureus* GatCAB guarantee accurate tRNA recognition. *Nucleic Acids Res.*, **38**, 672–682.
36. Rigaut,G., Shevchenko,A., Rutz,B., Wilm,M., Mann,M. and Seraphin,B. (1999) A generic protein purification method for protein complex characterization and proteome exploration. *Nat. Biotechnol.*, **17**, 1030–1032.
37. Danchin,A., Fang,G. and Noria,S. (2007) The extant core bacterial proteome is an archive of the origin of life. *Proteomics*, **7**, 875–889.
38. Giannouli,S., Kyritsis,A., Malissovas,N., Becker,H.D. and Stathopoulos,C. (2009) On the role of an unusual tRNA^{Gly} isoacceptor in *Staphylococcus aureus*. *Biochimie*, **91**, 344–351.